



## HARMONIC CURRENT COMPENSATION IN SELF EXCITED INDUCTION GENERATOR USING ACTIVE FILTER

Premalatha K<sup>1</sup>, Vasantharathna S<sup>2</sup>, Thirumoorthi P<sup>1</sup> and Yadaiah N<sup>3</sup>

<sup>1</sup> Department of Electrical and Electronics Engineering, Kumaraguru College of Technology, Coimbatore-641049.

Email : [kppremalatha@gmail.com](mailto:kppremalatha@gmail.com)

<sup>2</sup>Department of Electrical and Electronics Engineering, Coimbatore Institute of Technology, Coimbatore- 641014.

<sup>3</sup>Department of Electrical and Electronics Engineering, JNTUH College of Engineering, Hyderabad.

---

**Abstract:** The paper presents the concept of wind power generation system inverter as SAF under balanced and un-balanced conditions. PV based systems are practically inactive during the night time, Because of the system cannot conserve the energy on the night time. During the night time, the PV-SAF provides only the compensation for the reactive power disturbance through the battery bank. The reference currents extract by the Fuzzy logic controller based instantaneous active and reactive power (p-q) strategy. When the supply voltages are balanced and sinusoidal, then all controllers converge to the same compensation characteristics. However, when the supply voltages are distorted and/or un-balanced sinusoidal, these control strategies result in different degrees of compensation in harmonics. The p-q control strategy with PI controller is unable to yield an adequate solution when source voltages are not ideal. Extensive simulations were carried out; simulations were performed with balance, unbalanced and non sinusoidal conditions. Simulation results validate the dynamic behavior of Fuzzy logic controller over PI controller.

**Keywords:** Wind, Shunt Active Filter (W-SAF), conservation, P-Q Control, Fuzzy .

---

### 1. Introduction

Over the last two decades, renewable energy sources have been attracting attention due to the increasing cost, limited resources and adverse environmental impact of fossil fuels. Meanwhile, technological developments, cost reduction, less polluting, safety, quality of life and governmental incentives have made some renewable energy sources more competitive in the market. Among them, wind energy is one of the fast growing fields in renewable energy sources [1]. The induction generator is favored for small scale WECS because of its relative merits such as low capital cost, simplicity, robustness, absence of DC field power and small size per generated

power. Induction generators can be excited in either grid connected mode or self-excited mode. In grid connected mode, the required reactive power is drawn from the grid and the terminal voltage and frequency of the generator is constant at grid voltage and frequency. A lot of literature is available on the grid connected operation of induction generators and are presented in [2]-[7]. The SEIG is found more suitable for WECS in remote areas where it is difficult to install the transmission lines. In self-excited mode, required reactive power is supplied using fixed capacitor banks. The terminal voltage and frequency of the SEIG are not constant and depends on the wind speed, load impedance, power factor and excitation capacitance

value. In order to regulate the generator terminal voltage and frequency, VSC based controller is proposed. Nowadays, the use of nonlinear devices such as battery chargers, switched mode power supplies, UPSs, fluorescent lights etc. are increasing. These nonlinear devices draw non sinusoidal current from the SEIG and it contains fundamental component and harmonic components. These harmonic current components cause increased losses in the winding, torque pulsations on the shaft of the generator, quick aging of the materials and power quality problems. Harmonics can be effectively reduced through the use of passive filters, but it has some disadvantages. The disadvantages are it creates a parallel resonance at tuned frequency and a small variation in the value of inductance and capacitance alters the filtering characteristics [8-11]. Therefore, passive power filter would not be efficient for harmonic current compensation. To overcome the above problems shunt Active Power Filter (APF) is proposed. In the proposed work, the instantaneous active and reactive power theory (P-Q theory) is more suitable for shunt APF to determine the current reference and the DC voltage regulation is achieved using fuzzy logic controller (FLC). The FLC does not need accurate mathematical model, works with imprecise inputs and can able to handle parameter and load variations. The effectiveness and validity of the proposed FLC based shunt APF is verified through MATLAB simulation and experimental results.

The paper is organized as follows; Section I presents introduction to the subject. Section II gives modeling of the proposed system. Section III explains the control algorithm for reference current generation. Section IV presents the simulation results and discussions. Section V illustrates the experimental results. Finally, section VI concludes the work.

## 2. Proposed System

A schematic of the proposed WECS is shown in fig.1. The main parts of the proposed system are wind turbine, gear box, induction generator, capacitor bank and shunt APF. The shunt APF is conventionally built using VSC where it consists of six IGBTs with anti-parallel diodes for bidirectional current flow. The shunt APF is connected in parallel with nonlinear load. The DC side of APF is connected across a capacitor which maintains DC voltage constant. The delta connected capacitor bank is connected across the stator terminals to supply the initial reactive power for its excitation. The capacitance value is selected such that the SEIG produces rated terminal voltage at no load. When SEIG feeds a nonlinear load, the current supplied by the SEIG contains fundamental component and other harmonic components. The shunt APF is designed to minimize the harmonic components. The Shunt APF current is equal but opposite in-phase with the required harmonic component of load current. In the following sections, modeling of wind turbine, dynamic model of SEIG and then modeling of voltage source converter are presented.

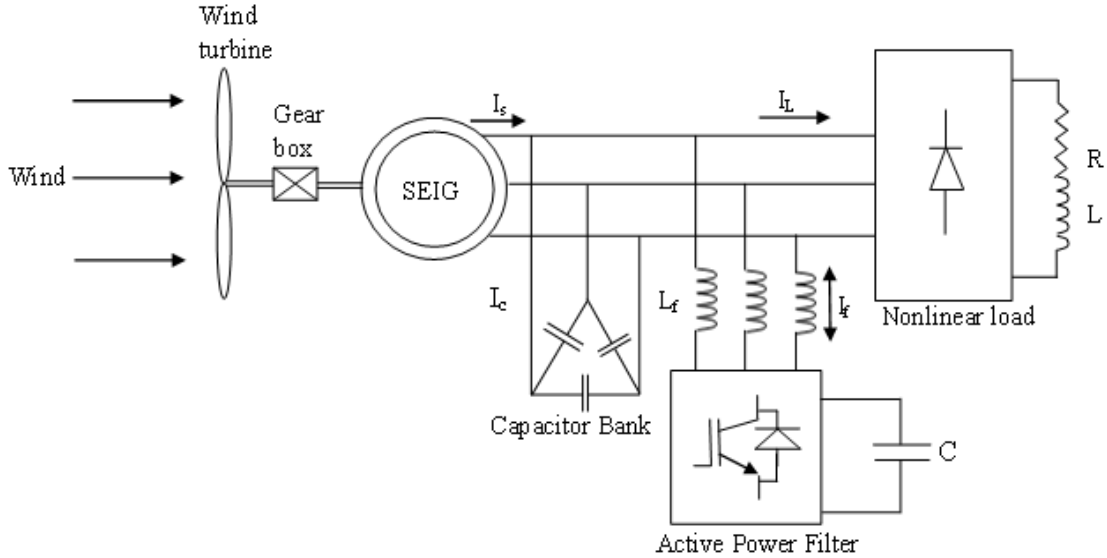


Figure 1. Block diagram of SEIG with shunt APF

### 2.1. Wind Turbine Model

The mechanical system consists of a wind turbine and gear. The gear ratio is selected such that the SEIG generates the rated voltage rated frequency at rated wind speed of 10m/s to extract the maximum power from the wind turbine. The aerodynamic power generated by the wind turbine is calculated from the following equation [7]

$$P_{wind} = \frac{1}{2} \rho_{air} A V^3 C_p \lambda, \beta \quad (1)$$

Where  $P_{wind}$  wind power,  $\rho_{air}$  - Specific density of air ( $kg/m^3$ ), A - Area of blades ( $m^2$ )

V - Wind speed (m/s),  $C_p$ - power coefficient which depends on the tip speed ratio  $\lambda$  of the wind turbine and  $\beta$  angle of blades.

### 2.2. Modeling of Induction Generator

Dynamic model of SEIG in arbitrary reference frame is obtained as [12]

Stator Voltage Equation

$$v_{ds} = R_s i_{ds} + \frac{d\psi_{ds}}{dt} - \omega_e \psi_{qs} \quad (2)$$

$$v_{qs} = R_s i_{qs} + \frac{d\psi_{qs}}{dt} + \omega_e \psi_{ds} \quad (3)$$

Rotor Voltage Equation

$$R_r i_{dr} + \frac{d\psi_{dr}}{dt} - \omega_e - \omega_r \psi_{qr} = 0 \quad (4)$$

$$R_r i_{qr} + \frac{d\psi_{qr}}{dt} + \omega_e - \omega_r \psi_{dr} = 0 \quad (5)$$

The electromagnetic torque developed by the induction generator can be calculated using equation (6)

$$T_e = \frac{3P}{2} \psi_{ds} i_{qs} - \psi_{qs} i_{ds} \quad (6)$$

### 2.3. Modeling of Voltage Source Converter

To simulate the three phase VSC, the switching function model is used. The phase voltages and current of a VSC on the AC side and DC side is computed using the DC link voltage and inverter gating signals  $S_a, S_b$  and  $S_c$  are given as

$$V_{an} = \frac{1}{3} (2S_a - S_b - S_c) V_{dc} \quad (7)$$

$$V_{bn} = \frac{1}{3} (2S_b - S_a - S_c) V_{dc} \quad (8)$$

$$V_{cn} = \frac{1}{3} (2S_c - S_a - S_b) V_{dc} \quad (9)$$

$$i_{dc} = S_a i_a + S_b i_b + S_c i_c \quad (10)$$

Where  $S_a$ ,  $S_b$  and  $S_c$  are switching functions stating the on/off positions of the switches. When  $S_a=1$ , upper switch of the inverter phase a leg is on and lower switch is off. While  $S_a=0$ , upper switch of the inverter phase a leg is off and lower switch is on. The similar logic is followed for other two phases also.

### 3. Harmonic Current Compensation

The control scheme for generating reference current is shown in fig.2. The reference current generation is based on the instantaneous active and reactive power (p-q) theory. The three phase generator terminal voltages ( $v_{sa}$ ,  $v_{sb}$  and  $v_{sc}$ ) and load currents  $i_{La}$ ,  $i_{Lb}$  and  $i_{Lc}$  are transformed to  $\alpha$ - $\beta$  reference frame using Clarke transformation is as follows [13,14].

$$\begin{bmatrix} v_\alpha \\ v_\beta \end{bmatrix} = \begin{bmatrix} -\frac{1}{2} & 1 & -\frac{1}{2} \\ \frac{\sqrt{3}}{2} & 0 & \frac{\sqrt{3}}{2} \end{bmatrix} \begin{bmatrix} v_{sa} \\ v_{sb} \\ v_{sc} \end{bmatrix} \quad (11)$$

$$\begin{bmatrix} i_{L\alpha} \\ i_{L\beta} \end{bmatrix} = \begin{bmatrix} -\frac{1}{2} & 1 & -\frac{1}{2} \\ \frac{\sqrt{3}}{2} & 0 & \frac{\sqrt{3}}{2} \end{bmatrix} \begin{bmatrix} i_{La} \\ i_{Lb} \\ i_{Lc} \end{bmatrix} \quad (12)$$

The instantaneous active power  $p$  and reactive power  $q$  of the load can be calculated as

$$\begin{bmatrix} p \\ q \end{bmatrix} = \begin{bmatrix} v_\alpha & v_\beta \\ -v_\beta & v_\alpha \end{bmatrix} \begin{bmatrix} i_{L\alpha} \\ i_{L\beta} \end{bmatrix} \quad (13)$$

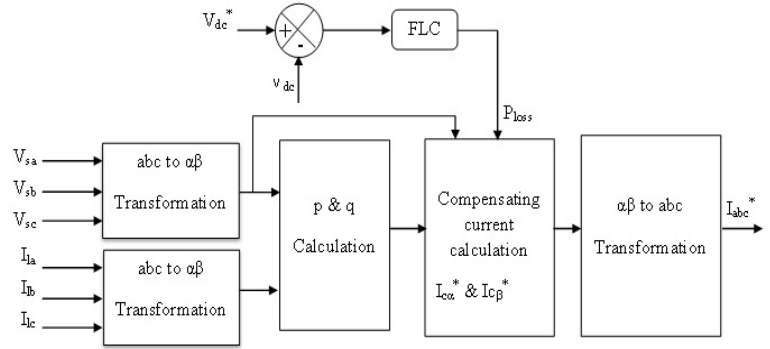


Figure 2. Control Scheme for reference current generation

The instantaneous power  $p$  and  $q$  delivered to load are normally divided into two components

Instantaneous active power

$$p = p_{dc} + p_{ac} \quad (14)$$

Instantaneous reactive power

$$q = q_{dc} + q_{ac} \quad (15)$$

$p_{dc}$  -DC component of active power and is supplied by the generator which is related to instantaneous fundamental active power of the load.

$p_{ac}$  - AC component of active power and is associated with harmonic power of the load.

$q_{dc}$  - DC component of reactive power and is generated by fundamental voltages and currents.

$q_{ac}$  - AC component of reactive power and is equal to conventional reactive power.

#### 3.1. Dc Voltage Control

The DC link voltage is controlled by a FLC controller and it generates a signal, ( $P_{loss}$ ) which is the instantaneous real power required to control the DC link voltage. The inputs to FLC are the error between the measured DC link voltage and the reference dc link voltage ( $e=V_{dc}^* - V_{dc}$ ) and the change of error ( $\Delta e=e(n)-e(n-1)$ ). The output of the fuzzy logic controller is considered as the active power ( $P_{loss}$ ) and it supplies converter losses and active power demand of the load.

### 3.1.1. Fuzzy Control Algorithm

Fuzzy logic allows the modeling of complex systems using knowledge and experience. The output is obtained for the given input without using any mathematical equations, but by using linguistic rules. The structure of the FLC is shown in fig.3. The main actions performed by a FLC are fuzzification, evaluation of control rules and defuzzification.

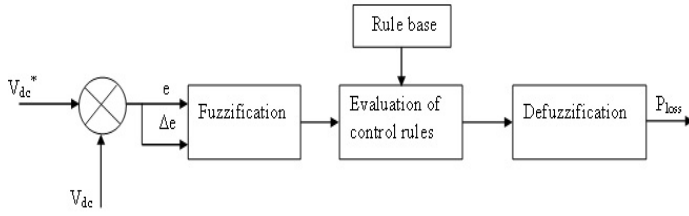
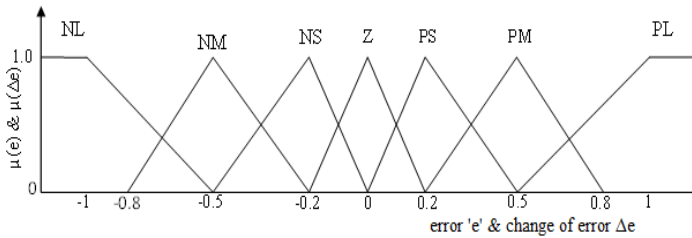
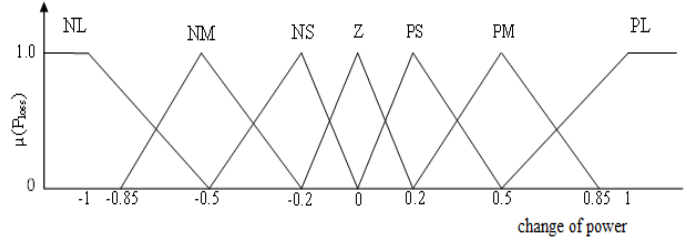


Figure 3. Structure of FLC

The DC voltage error and change of error are given as crisp inputs to the FLC and are transformed into linguistic variables using membership functions. The membership functions for error (e), change of error (Δe) and change of active power (P<sub>loss</sub>) are shown in fig.4. There are seven triangular MFs for the input and output and are NL (negative big), NM (negative medium), NS (negative small), Z (zero), PS (positive small), PM (positive medium), NL (positive big). The fuzzy rules are constructed using knowledge data base. The rule base for FLC is presented in Table-I. There are 49 rules and are used to determine the output. Finally, the output is defuzzified using center of gravity method. The crisp output of FLC is P<sub>loss</sub>.



(a)



(b)

Figure 4. Membership functions for error, change of error and change of power

Table 1. Fuzzy Rule Base

e Δe	NB	NM	NS	Z	PS	PM	PB
NB	NB	NB	NB	NB	NM	NS	Z
NM	NB	NB	NB	NM	NS	Z	PS
NS	NB	NB	NM	NS	Z	PS	PM
Z	NB	NM	NS	Z	PS	PM	PB
PS	NM	NS	Z	PS	PM	PB	PB
PM	NS	Z	PS	PM	PB	PB	PB
PB	Z	PS	PM	PB	PB	PB	PB

### 3.2. Calculation Of Reference Compensating Current

The reference power needed for reactive power and harmonic current compensation after eliminating all the harmonic components by low pass filter are given by  $p_{ref} = p + P_{loss}$  and  $q_{ref} = q$ . The calculated reference values are used to obtain the compensating currents in  $\alpha$ - $\beta$  coordinates and are given by

$$\begin{bmatrix} i_{c\alpha}^* \\ i_{c\beta}^* \end{bmatrix} = \frac{1}{v_\alpha^2 + v_\beta^2} \begin{bmatrix} v_\alpha & v_\beta \\ v_\beta & -v_\alpha \end{bmatrix} \begin{bmatrix} p_{ref} \\ q_{ref} \end{bmatrix} \quad (16)$$

The instantaneous reference compensating currents in a-b-c reference frame are calculated from inverse transformation shown in the relation (17) given below [13, 14]

$$\begin{bmatrix} i_a^* \\ i_b^* \\ i_c^* \end{bmatrix} = \begin{bmatrix} 1 & 0 \\ 2 & -1 \\ 3 & 2 \end{bmatrix} \begin{bmatrix} 0 \\ 3 \\ 2 \end{bmatrix} \begin{bmatrix} i_{c\alpha}^* \\ i_{c\beta}^* \end{bmatrix} \quad (17)$$

### 3.3. Hysteresis Current Controller

Among the various current control techniques, hysteresis current control scheme is the simplest and most extensively used technique. The main advantages of hysteresis current control are simplicity, lack of tracking errors, independence of load parameter changes and fast response. In this approach, the actual source currents are compared with the reference currents generated by the algorithm. The resulting current error is fed to the hysteresis current controller to determine the gating signals for the switches of the converter. The switching logic for the voltage source converter is as follows: If  $i_{sa} > (i_a^* + hb)$ , the upper switch of the phase 'a' leg is ON and lower switch is OFF. If  $i_{sa} < (i_a^* - hb)$ , the upper switch of the phase 'a' leg is OFF and lower switch is ON, where  $hb$  is the bandwidth of the hysteresis controller. The similar logic is followed for other two phases also.

### 4. Simulation Results

Fig. 5-7 shows the simulation results of the proposed system. The simulation is carried out on 400V, 10hp delta connected squirrel cage induction generator driven by the wind turbine. The generator is excited by delta connected capacitor banks. The capacitor value of ( $24\mu\text{F}/\text{phase}$ ) is needed to produce a no load voltage of 400V. The parameters of the generator and filter are presented in appendix. The performance of the shunt APF is studied for SEIG driven by a wind turbine of constant power feeding nonlinear load. The generator terminal voltage, source current, load current and filter current waveforms are shown in fig.5. Fig.6. shows the harmonic spectrum of the source current without filter which has a THD value of 29.61%. Fig.7. shows the harmonic spectrum of source current with filter and its THD value is 4.78%. After source current compensation the voltage and current are in phase and the power factor is unity.

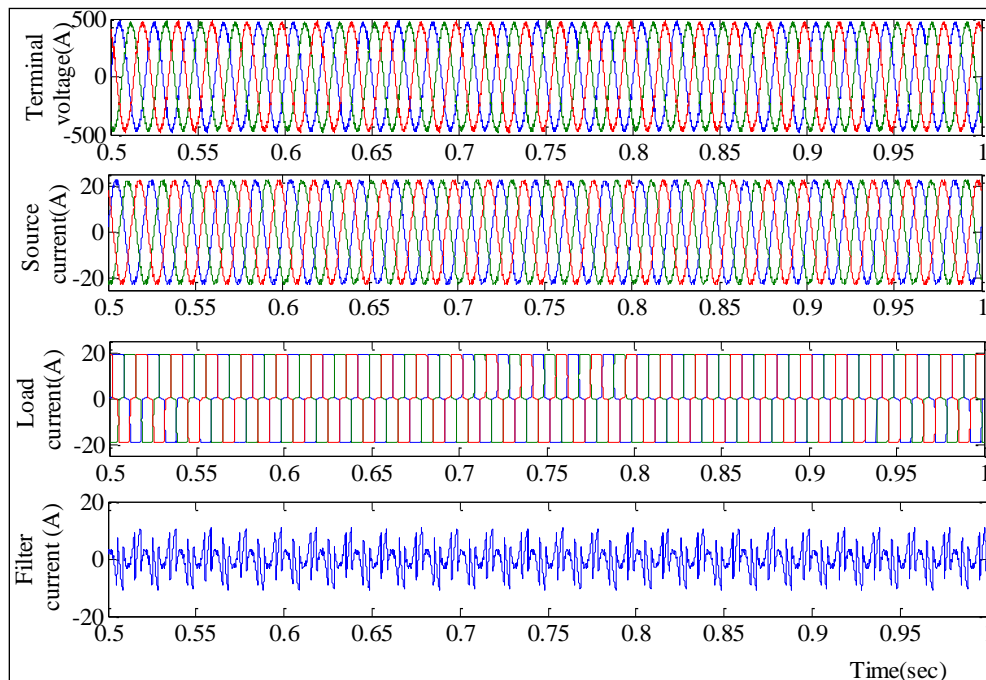
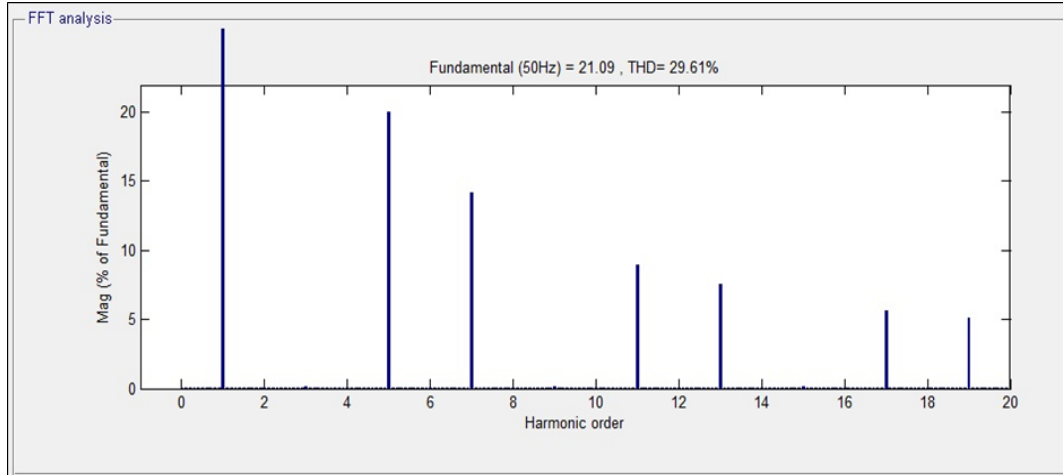
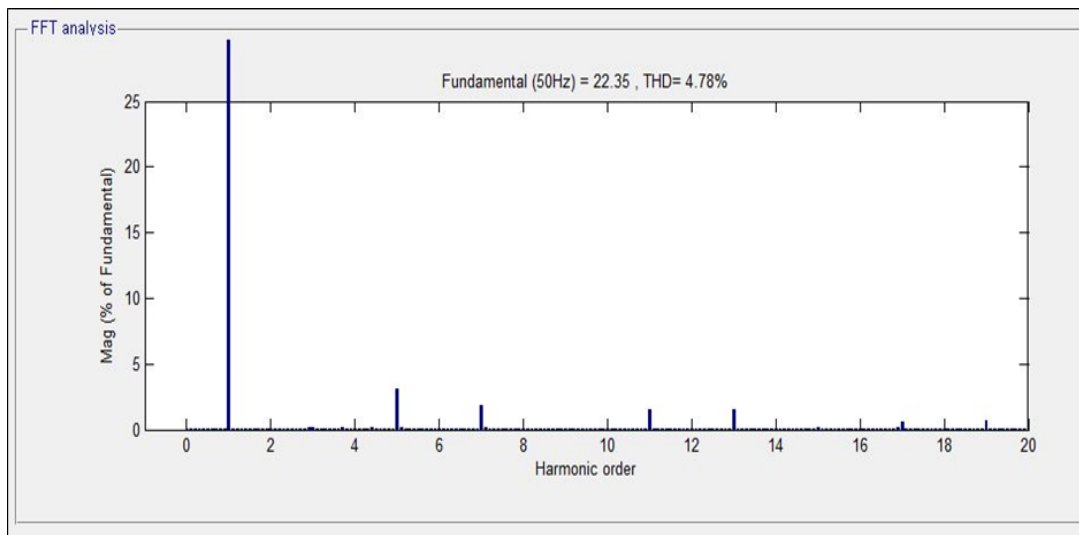


Figure 5. Simulation results of the proposed system for constant load



**Figure 6.** Harmonic spectrum of the source current without filter



**Figure 7.** Harmonic Spectrum of the source current with filter

## 5. Experimental Results

A laboratory prototype model of the proposed Shunt active filter for WECS is developed and tested to validate the simulation results. The hardware model is developed using 0.5kW, 100V delta connected, 4 pole SEIG with Capacitor bank of 250VAR, VSC, DC bus capacitor, filter inductors and interfacing circuits. A Field Programmable Gate Array (FPGA) is used to generate the switching pulses of VSC using the control algorithm. The Induction machine parameters are

obtained by conducting no load and blocked rotor tests ( $R_s = 8\Omega$ ,  $R_r = 6.8\Omega$ ,  $L_{ls} = L_{lr} = 30\text{mH}$  and  $L_m = 250\text{mH}$ ). The diode rectifier with resistive and inductive load is used to determine the effectiveness of the shunt APF. The shunt APF is not connected source current is distorted. The shunt APF is switched on; under steady state the source current is sinusoidal and is in phase with the source voltage.

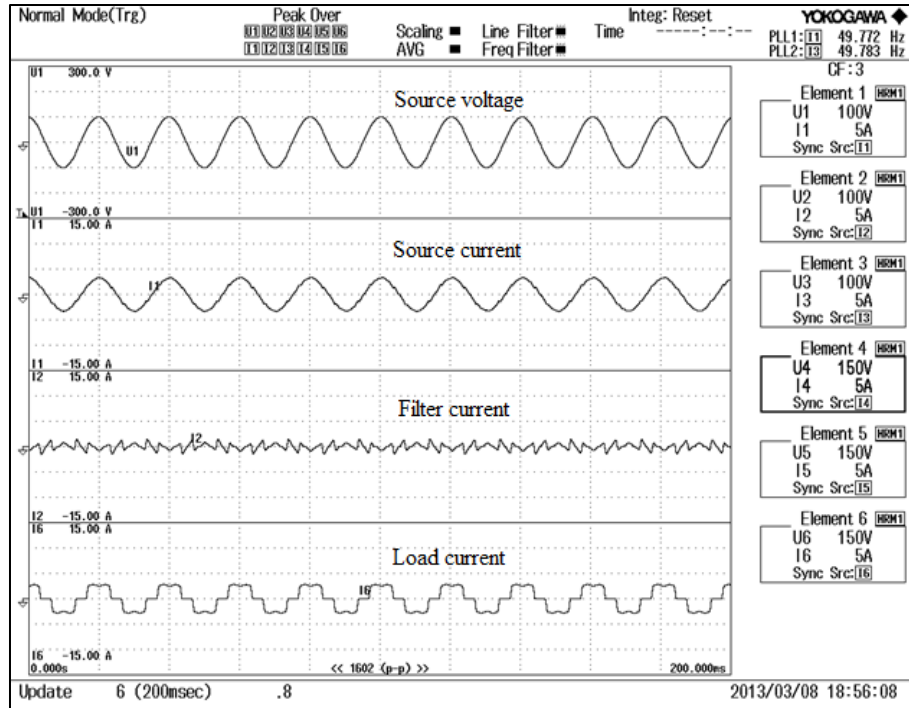


Figure 8. Experimental results of source voltage, source current, filter current and load current

## 6. Conclusion

A laboratory prototype model of shunt active filter for wind turbine driven SEIG feeding nonlinear load has been implemented and its performance is analyzed. It has been observed that, improved generator current waveform and its Total Harmonic Distortion is reduced to 4.78%. The simulation and experimental results are presented to validate the control algorithm. The proposed control algorithm is simple and has fast dynamic response. The shunt active filter has been found more suitable to eliminate the current harmonics in the SEIG and the resulting generator current is sinusoidal.

## Appendix

### A.1. Induction Machine Parameters

10 hp, 400V,  $\Delta$  connected, 4 pole, 50Hz, 1440 rpm,  $R_s=4.34\Omega$ ,  $R_r=3.89\Omega$ ,  $L_s = L_r= 210\text{mH}$ ,  $L_m= 195\text{mH}$ .

### A.2. Nomenclature

$P_{\text{wind}}$	Wind power (W)
$\rho$	Specific density of air ( $\text{kg/m}^3$ )
$A$	Area of blades ( $\text{m}^2$ )
$C_p$	Power coefficient of the wind turbine
$V$	Wind speed (m/s)
$\beta$	Angle of blades
$v_{ds}$ and $v_{qs}$	d- axis and q-axis stator voltages (V)
$i_{ds}$ and $i_{dr}$	d- axis stator and rotor currents (A)
$i_{qs}$ and $i_{qr}$	q-axis stator and rotor currents (A)
$\psi_{ds}$ and $\psi_{qs}$	d- axis and q-axis stator flux linkages
$\psi_{dr}$ and $\psi_{qr}$	d- axis and q-axis rotor flux linkages
$R_s$ and $R_r$	Stator and rotor resistances ( $\Omega$ )
$\omega_r$	Rotor speed (rad/sec)
$\omega_e$	Stator supply frequency (rad/sec)
$v_s$	Generator terminal voltage (V)
$i_l$	Load current (A)
$V_{dc}$	DC link voltage (V)
$i^*$	Reference current (A)

## 7. References

- [1] Wu, B., Lang, Y., Zargari, N., and Kouro, S., *Power Conversion and Control of Wind Energy Systems*, John Wiley & Sons, 2011.
- [2] Jose Luis D G., Oriol GB., Lluís T R., and Adria J F., “Indirect Vector Control of a Squirrel Cage induction generator wind turbine”, *Computers and Mathematics with Applications*, Elsevier, Vol:64, No: 2, pp. 102-114, 2012.
- [3] Roberto C., Ruben P., Jon C., and Patrick W., “Analytical and Experimental Evaluation of a WECS based on a cage Induction generator fed a Matrix Converter”, *IEEE transactions on Energy Conversion*, Vol:26, No:1, pp. 204-215, 2011.
- [4] Tolga S., and Eyup A., “Modeling of a 5kW WECS with induction generator and comparison with experimental results”, *Renewable Energy Journal*, Vol: 30, pp.913-929, 2005.
- [5] Gabriel C., and Stefan B., “Design and control strategies of an Induction machine based fly wheel energy storage system associated to a variable speed wind generator”, *IEEE transactions on Energy Conversion*, Vol: 25, No: 2, pp.526-534, 2010.
- [6] Blaabjerg F., Chen Z., Teodorescu R., and Lov F., “Power Electronics in Wind Turbine Systems”, *Proceedings of International Conference on Power Electronics and Motion Control, Shanghai, China*, pp. 1-11, 2006.
- [7] Vladislav A., *Induction Generators for Wind Power*, Multi-Science Publishing Co. Ltd, UK, 2005.
- [8] Darwin R., Luis M., Juan D., and Jose E., “Improving passive filter compensation performance with active Techniques”, *IEEE transactions on Industrial Electronics*, Vol: 50, No: 1, pp. 161-168, 2003.
- [9] Akagi H., Watanabe E. H., and Aredes M., *Instantaneous Power Theory and Applications to Power Conditioning*, Piscataway, NJ: IEEE Press, 2007.
- [10] Buso S., Malesani L., and Mattavelli P., “Comparison of current control techniques for Active Power Filter Applications”, *IEEE transactions on Industrial Electronics*, Vol: 45, No:5, pp. 722-729, 1998.
- [11] Tsengenes G., and Georgios A., “Shunt Active Power Filter Control Using Fuzzy Logic Controllers”, *Proceedings of International Symposium on Industrial Electronics*, Poland, pp 365-371, 2011.
- [12] Krause P.C., Wasynczuk O., and Sudhoff S.D., *Analysis of Electric Machinery and Drive Systems*, IEEE press, NewYork, 2002.
- [13] Mikko R., Mika S., and Heikki T., “Comparison of Voltage-Source and Current-Source Shunt Active Power Filters”, *IEEE Transactions on Power Electronics*, Vol: 22, No: 2, pp. 636-643, 2007.
- [14] Carneiro H., Couto C., and Afonso, J.L., “Simulations of a current-source Shunt Active Power Filter with Carrier-Based PWM and Periodic Sampling modulation techniques Power Electronics and Applications”, *Proceedings of International Conference on Power Electronics and Applications*, Birmingham, pp. 1-8,2011.